Available online at www.sciencedirect.com

SCIENCE DIRECT®

Journal of Electroanalytical Chemistry

Journal of Electroanalytical Chemistry 554–555 (2003) 49–60

www.elsevier.com/locate/jelechem

In situ FTIRRAS study of the electro-oxidation reactions of thiourea and gold in aqueous acid solutions

A.E. Bolzán [a,*], T. Iwasita [b], A.J. Arvia [a]

[a] *Instituto de Investigaciones Fisicoquímicas Teóricas y Aplicadas (INIFTA) (UNLP, CONICET), Sucursal 4, Casilla de Correo 16, (1900) La Plata, Argentina*

[b] *Instituto de Quimica de São Carlos, Universidade de São Paulo, Sao Carlos, Brazil*

Received 21 October 2002; received in revised form 15 December 2002; accepted 4 January 2003

Abstract

The electro-oxidation of gold and thiourea (TU) in aqueous acid solutions is investigated by means of in situ FTIRRAS measurements complemented by voltammetry. The formation of soluble species related to the gold(I)–TU complex and TU electro-oxidation products is monitored by following the changes in the IR spectra with the applied potential in the range −0.1–1.5 V. Experimental data show that gold electrodissolution produces soluble $[Au(CS(NH_2)_2)_2]_2SO_4$ species. The IR spectrum of solid samples of this complex is reported. The electrodissolution reaction begins at approximately 0.15 V (SHE), concomitantly with the early stages of TU electro-oxidation. The electro-oxidation of TU on gold in acid solutions produces formamidine disulphide (FDS) at potentials below 1.2 V (SHE). The formation of the gold complex and that of FDS are quasi-reversible processes, as revealed by FTIRRAS data. Once the formation of the oxygen-containing layer on gold sets in, the electro-oxidation of TU and FDS yields carbon dioxide, sulphate ions and CN-containing products. Adsorbed sulphate species, which are also detected from 1.2 V upwards, exhibit a band shift of 27 cm^{-1} V^{-1}.

Keywords: Thiourea; Electro-oxidation; Formamidine disulphide; FTIRRAS; Gold; Electrodissolution

1. Introduction

Thiourea (TU) is a relatively small molecule that is used for different purposes of technological interest. At low concentration, it acts as an inhibitor to prevent the corrosion of active metals such as iron [1] and copper [2,3], as a catalyst for the electroreduction of metal ions such as Zn(II) and Cd(II) [4,5] or as an additive for electrolytically driven lattice formation processes such as in copper deposition [6]. On the other hand, at high concentration, TU appears as a promising extracting agent of precious metals from their ores [7–9], because of its complex forming capability. In the case of gold, it results in the formation of complex salts containing the $[Au(TU)_2]^+$ cation. The syntheses of this complex cation as bromide [10], chloride [11] and sulphate [11] salts and their structures, determined by X-ray diffraction, have been reported.

The specific adsorption and electroadsorption of TU on different metal surfaces, including gold, are very strong, as is concluded from surface enhanced Raman spectroscopy [12–14] and electrochemical techniques [14–16]. There is general agreement that in these processes the main gold–TU interactions occurs via the sulphur atom [14,17]. Radiotracer data have been used to determine the range of potentials related to the stability of TU adsorbates on gold [18]. At potentials more negative than those where TU electroadsorption takes place, there is evidence of sulphiding of the gold electrode, whereas at the positive potential side, adsorbate electro-oxidation produces a number of byproducts [18].

The anodic oxidation of TU in aqueous acid solutions either on platinum [19], copper [20] or gold [16], exhibits a first quasi-reversible stage related to the formation of formamidine disulphide (FDS) as the main product.

* Corresponding author. Fax: +54-221-4254642.
E-mail address: aebolzan@inifta.unlp.edu.ar (A.E. Bolzán).

0022-0728/03/$ - see front matter
doi:10.1016/S0022-0728(03)00050-0

FDS is also produced relatively easily by homogeneous reactions in solution between TU and oxidants such as hydrogen peroxide [21]. In any case, FDS can be further oxidised to either elemental sulphur or sulphate ions [22,23] and cyanamide [23]. The formation of carbon dioxide from TU electro-oxidation has also been proposed [16]. In fact, it is known that FDS in aqueous acids is unstable and decomposes irreversibly into cyanamide and elemental sulphur [22].

The electrodissolution of gold in aqueous TU-containing acid solutions proceeds with 100% efficiency for $E < 0.3$ V (SHE), while for $E > 0.3$ V the reaction is accompanied by TU electro-oxidation to FDS and other byproducts [24]. Correspondingly, the efficiency of gold electrodissolution decreases. TU electro-oxidation to FDS either precedes or at least occurs concomitantly with the electrodissolution of gold, depending on the concentration of TU [16]. The latter occurs even in the potential range related to the formation of the oxygen-containing layer on gold. In the potential range of this process, strongly bound adsorbates produced from TU are also electro-oxidised, seemingly yielding sulphate and carbon dioxide as the main products [16]. This agrees, to some extent, with the presence of sulphur octomers at potentials beyond the formation of FDS adsorbates on Au (1 1 1), which has been detected by STM imaging [25].

In spite of increasing interest in the gold | TU aqueous interface, no in situ identification of the reaction products has been attempted. In fact, in situ spectroscopic techniques have mostly been applied to study TU adsorption on gold and the resulting adsorbate structures [14,25]. FTIRRAS can be considered as a suitable tool to identify and follow the in situ evolution of reactants and products involved in the complex reaction system encountered at the gold | aqueous TU electrochemical interface [23,26–28]. In fact, this technique has been used to monitor the adsorption of TU on copper [29], iron [26] and silver [28] and its electro-oxidation on platinum [23].

In the present work the simultaneous electro-oxidation of polycrystalline gold and TU in aqueous acid solutions was investigated with the aim of identifying reactants and products, and changes of their concentration at the metal | solution interface. Attention was also paid to the formation of gold–TU complex species.

2. Experimental

In situ FTIRRAS experiments were performed using a Nicolet Nexus 670 spectrometer equipped with a liquid nitrogen cooled MCT detector. The spectroelectrochemical cell was fitted with a 60° prismatic calcium fluoride window. The working electrode was a mirror-polished gold disk 0.7-cm in diameter. Before each run it was mechanically polished with alumina 0.3-μm grit and rinsed with acetone and Milli-Q water. A reversible hydrogen electrode was used as the reference electrode and a gold foil surrounding the working electrode was employed as the counter electrode.

Normalised reflectance spectra were calculated as R/R_0, where R is the value of the reflectance at the sampling potential E_s and R_0 is the reflectance measured at a reference potential E_{ref}. The value of E_{ref} was set slightly below the rest potential of gold in the working solution, i.e., a value where TU electro-oxidation is precluded, in order to follow the formation of electro-oxidation products. Occasionally, the electrode was immersed at a sufficiently negative ($E_{ref} = -0.1$ V) or positive ($E_{ref} = 0.3$ V) potential, that allowed us to establish well-defined reduction and oxidation reference states and follow the appearance and disappearance of soluble products during the initial stages of TU and gold electro-oxidation. Accordingly, positive- and negative-going absorption bands in the spectra represent the loss and gain of species at E_s as compared to E_{ref}, respectively. At each sampling potential, either 256 or 512 interferograms with 8 cm^{-1} resolution were computed. Parallel (p) and perpendicular (s) polarised light was obtained from a barium fluoride supported aluminium-wire grid polariser. For the FTIRRAS experiments, the electrode potential was controlled by means of a Wenking potentiostat and a potential step generator.

Attenuated total reflection (ATR) spectra were obtained for TU and FDS in aqueous 0.1 M perchloric acid using a germanium prism. The background spectra were recorded by adding 0.1 ml of aqueous 0.1-M perchloric acid. Subsequently, 0.1 ml of either aqueous 0.1 M TU or 0.1 M FDS+0.1 M perchloric acid was added to record the ATR spectra of TU and FDS, respectively.

The IR spectrum disk-shaped solid sample corresponding to $[Au(TU)_2]_2SO_4$ and potassium bromide was determined in the region 4000–400 cm^{-1} by means of a Shimadzu spectrometer. For this purpose, the complex salt was prepared as indicated elsewhere [11].

Complementary voltammetric runs were performed utilising a conventional three electrode cell with a polycrystalline gold wire working electrode (0.25 cm^2 geometric area, J. Matthey, spec pure), a large platinum sheet (2 cm^2 apparent area) as the counter electrode, and a mercurous sulphate electrode, as the reference. The working electrode was polished mechanically with alumina and rinsed with Milli-Q water before each experiment. For these measurements, the electrochemical setup consisted of an LYP potentiostat coupled to a waveform generator.

Working solutions were prepared from TU (Fluka, puriss.), FDS dihydrochloride (FDS·2HCl, ICN, 97%), sulphuric acid (97% Merck, p.a.), perchloric acid (70% Merck, p.a.) and either Milli-Q water or deuterium

oxide (Aldrich, 99.9%). The latter was employed to study the FTIRRAS spectra in the region where water bands obscure the presence of those related to TU and FDS. All solutions were saturated with nitrogen before the experiments.

All the experiments were performed at room temperature.

3. Results and interpretation

3.1. Voltammetry

The voltammogram of gold in aqueous 0.1 M TU + 0.5 M sulphuric acid at 0.05 V s^{-1} (Fig. 1a) shows a small anodic peak (Ia) at approximately 0.46 V and a large anodic peak (IIa) at 0.9 V. Peak IIa is followed by an anodic current with a hump (peak IIIa) at approximately 1.2 V (peak IIa/IIIa height ratio >1). Then, the anodic current decreases slowly as E approaches 1.6 V. The subsequent reverse scan shows a quasi linear decrease in the anodic current from 1.6 to 1.3 V, peaks IIIa and IIa which are overlapped to a great extent, and exhibit a current ratio (IIa/IIIa) <1. From 0.6 to 0.2 V, the anodic current becomes almost constant, and finally cathodic peak Ic at 0.12 V and hump IIc at approximately 0 V are recorded.

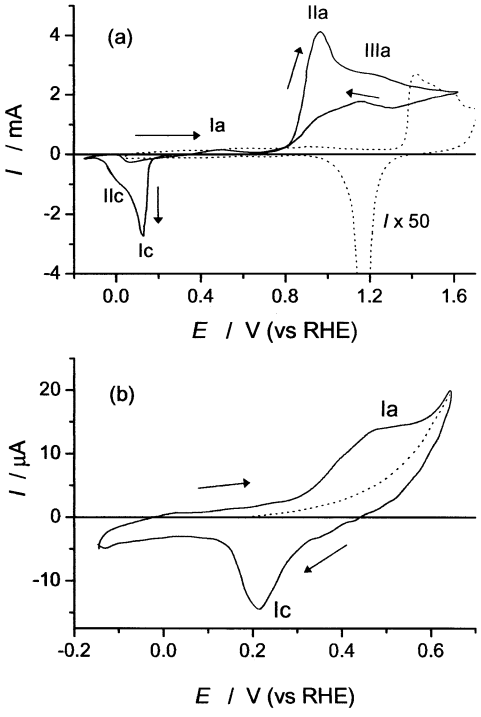

Fig. 1. (a) Voltammograms of gold in 0.5 M sulphuric acid (dashed line) and 0.1 M TU + 0.5 M sulphuric acid (full line) run between −0.2 and 1.65 V. (b) Voltammogram of gold in 0.1 M TU + 0.5 M sulphuric acid run between −0.2 and 0.65 V; the dashed line shows the extrapolation of peak IIa to $I=0$. $v=0.05$ V s^{-1}.

In the range between −0.15 and 0.65 V, the voltammogram (Fig. 1b) shows conjugated peaks Ia at approximately 0.45 and Ic at approximately 0.22 V. This pair of peaks is related to the TU/FDS redox couple [16,19,30]. After peak Ia, the anodic current starts to increase due to the electrodissolution of gold. This process is responsible for the appearance of peak IIa (Fig. 1a), but the formation of soluble gold complexes presumably started at lower potentials concomitantly with the formation of FDS from TU. This assertion is supported by data from the extrapolation to $I \rightarrow 0$ of the faradaic current related to peak IIa (Fig. 1b), and it agrees with the prediction of the potential–pH aqueous solution diagrams for the gold–TU–water system [31], indicating that for 0.1 M TU + 10^{-6} M gold ion in 0.5 M sulphuric acid, the formation of soluble gold complex species should occur at approximately 0.22 V [31]. It should be noted that the stability domain for gold complexes depends on both the gold ion and TU concentration (c_{TU}). Thus, it becomes smaller either on increasing gold ion concentration at constant c_{TU} or increasing c_{TU} at constant gold ion concentration [31].

To confirm that peaks Ia and IIa are related to the electro-oxidation of TU to FDS and to gold electrodissolution, respectively, voltammograms restricted to the potential range of either peak Ia or peak IIa were obtained (Fig. 2). For peak Ia, on reversing the potential scan at approximately 0.45 V (Fig. 2a) the decrease in current that should be expected for a pseudocapacitive process is observed prior to peak Ic. But, when the voltammetric run is extended to the potential range of

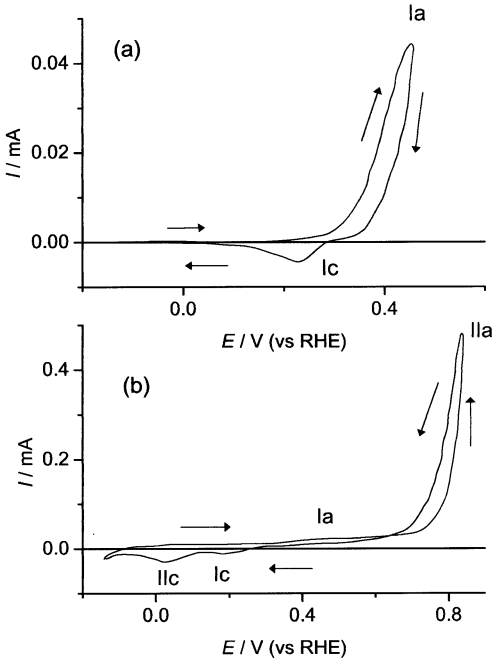

Fig. 2. Voltammograms of gold in 0.1 M TU + 0.5 M sulphuric acid run between −0.2 and 0.45 V. (a) and −0.2 and 0.83 V (b) $v=0.05$ V s^{-1}.

peak IIa (Fig. 2b), the reverse scan shows an anodic current loop that resembles those usually observed for metal electrodissolution in aggressive environments. Nevertheless, voltammetric data are consistent with the main processes associated with peaks Ia and IIa referred to above, although this does not preclude the possibility that the chemical dissolution of gold by TU at lower potentials may be suppressed. As is shown further on, the formation of gold soluble complexes is feasible even in the potential range of peak Ia.

On the other hand, a voltammogram run at 0.005 V s^{-1} (Fig. 3) shows successive anodic peaks, namely, peak Ia at approximately 0.44, peak IIa at approximately 0.92 V, hump IIIa at approximately 1.2 V, and peak IVa at approximately 1.40 V. During the reverse potential scan, the anodic current decreases to a minimum at 1.37 V, then it rises to hump IIIa and decreases again rather rapidly showing a hump close to the potential of peak IIa, and eventually attains a rather constant current from approximately 0.6 to 0.3 V. The voltammograms run at the lowest potential scan rate show no cathodic current peak. Therefore, peak Ic and hump IIc, which are observed at higher scan rates, should be related to the electroreduction of soluble species produced from both TU and gold electrooxidation reactions. These products diffuse away from the reaction interface and are not detected at v sufficiently low. In fact, similar experiments with decreasing v show a gradual decrease in the cathodic current contribution in the 0.4–0.0 V range, as v is decreased.

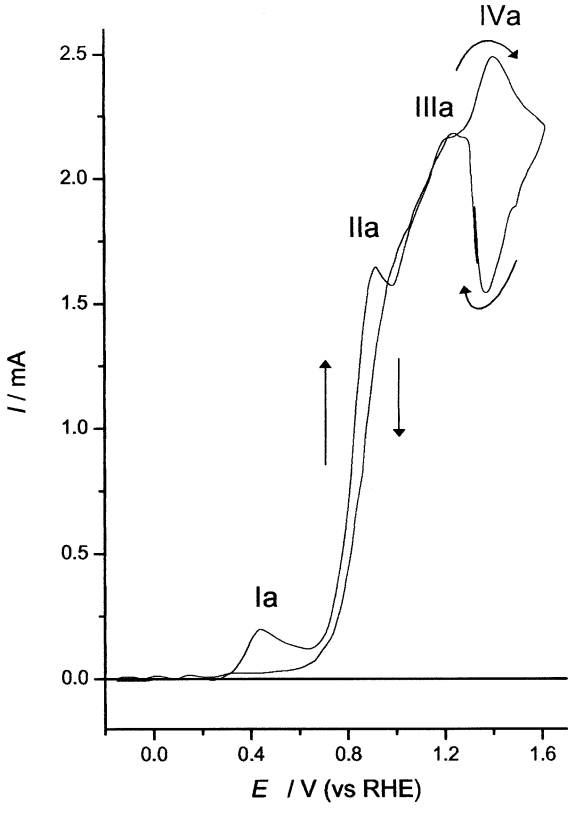

Fig. 3. Voltammograms of gold in aqueous 0.1 M TU+0.5 M sulphuric acid run between −0.2 and 1.65 V. $v = 0.005$ V s^{-1}.

3.2. ATR spectra of TU and FDS in 0.1 M aqueous perchloric acid

ATR spectra of TU and FDS in aqueous 0.1 M perchloric acid as well as that of aqueous 0.1 M perchloric acid (blank) were measured in the range 1000–2000 cm^{-1}. The spectrum of TU (Fig. 4a) shows a band at 1100 cm^{-1} related to the asymmetric stretching of perchlorate ion, and two bands at 1405 cm^{-1}, due to CN and CS stretchings and NH_2 rocking modes [23], and 1627 cm^{-1} due to the bending of the NH_2 group of TU [23].

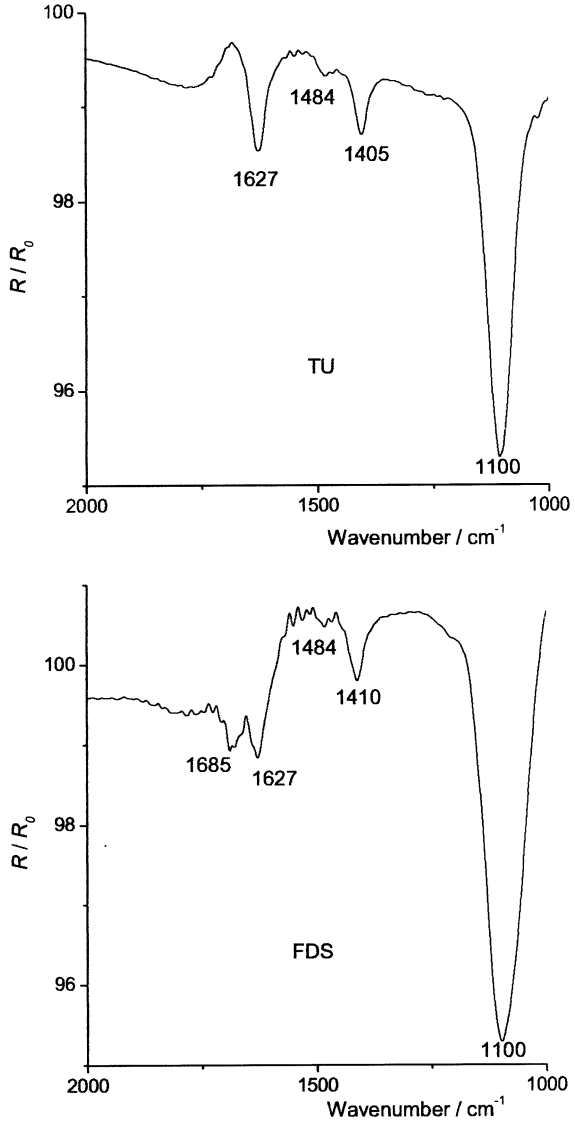

Fig. 4. ATR spectra obtained for (a) 0.1 M TU+0.1 M perchloric acid and (b) 0.1 M FDS+0.1 M perchloric acid.

The spectrum of FDS (Fig. 4b) shows bands at 1100, 1410, 1627 and 1685 cm^{-1}. The FDS bands are slightly blue-shifted as compared to that of TU. For FDS in Nujol [32], absorption bands at 1400, 1630 and 1654 cm^{-1} have been reported. They were assigned to the stretching of the CN_2 and C–S bonds and rocking of the NH_2 group (1400 cm^{-1}), bending of NH_2 and stretching of CN_2 groups (1630 cm^{-1}), and bending of the NH_2 group (1654 cm^{-1}).

3.3. IR spectrum of solid $[Au(TU)_2]_2SO_4$ in KBr

It has recently been found that the dissolution of gold in TU-containing acid solutions produces a soluble gold(I)–TU complex ion (hereafter simply denoted as a gold complex) of formula $(Au[TU]_2)^+$ [16]. The IR spectrum of the sulphate salt of this complex ion is reported here for the first time. This spectrum will be used as a guide for identification of soluble gold-containing products during anodisation at different potentials in TU-containing acid solutions.

For this purpose, the IR spectrum of $(Au[TU]_2)_2SO_4$ was measured using a potassium bromide disk. The resulting spectrum for the spectral region 400–2000 cm^{-1} is depicted in Fig. 5. By comparing the absorption bands exhibited by the gold complex with those reported for TU (Table 1), the following tentative assignments can be advanced. The medium band at 709 cm^{-1} is likely to be due to the C–S stretching that for pure TU appears at 753–758 cm^{-1} (Tables 1 and 2). The red shift of this band is similar to that found for copper(I)–TU complexes [33] (Table 2). The weak band at 1052 and the strong band at 1089 cm^{-1} can be associated with rocking modes of NH_2 groups and stretching modes of the CN_2 group [32], while those strong bands appearing in the range 1391–1495 cm^{-1} should be mainly due to the stretching of C–S and C–N bonds. The strong band at 1434 cm^{-1} is most interesting as it agrees with that found during the electro-oxidation of gold in TU-containing acid solutions, as described in the next section. Finally, the three strong overlapping bands at 1591, 1615 and 1629 cm^{-1} can be assigned to bending modes of the NH_2 groups. The band appearing at 1180 cm^{-1} is likely to be related to sulphate in the complex salt.

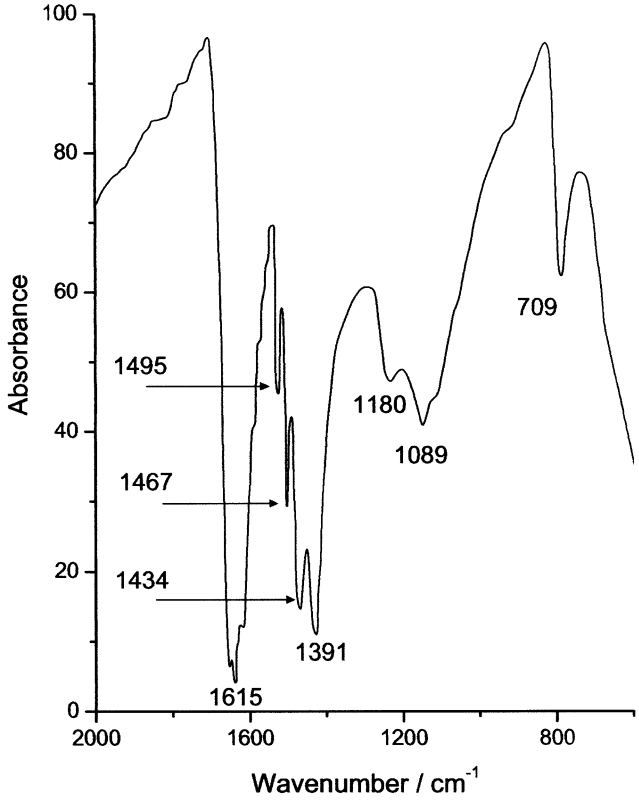

Fig. 5. IR spectrum of solid $(Au[TU]_2)_2SO_4$ in a KBr disk.

Table 1
Principal infrared bands of TU

Frequency/cm^{-1}	Assignment	References
1040	$\rho NH_2+\nu_{as}CN_2$	[32]
1083s	$\rho NH_2+\nu_{s}CN_2$	[32]
1083	$\nu NCN+\rho NH_2+\nu CS$	[53]
1084	$\nu CN+\rho NH_2$	[46]
1086m	$\nu_5(\rho NH)_{a1}+\nu_{17}(\rho NH)_{b2}$	[54]
1088	$\rho NH_2+\nu_5CN_2$	[47]
1407s	$\nu CS+\nu CN$	[55]
1413vs	$\nu CN_2+\rho NH_2+\nu CS$	[32]
1413s	$\nu_4(\nu CS)_{a1}$	[54]
1414	$\nu CN+\delta NH_2+\Delta NCN+\nu CS$	[46]
1415	$\nu_5CN_2+\nu CS+\rho NH_2+\delta NH_2+\delta CN_2$	[47]
1417	$\delta NH_2+\nu NCN+\nu CS$	[53]
1470	νNCN	[53]
1470s	$\nu CS+\nu CN$	[55]
1472vs	$\nu_{as}CN_2+\delta NH_2$	[32]
1473s	$\nu_{16}(\nu CN)_{b2}$	[54]
1473	νCN	[46]
1588vs	$\delta NH_2+\nu_{as}CN_2$	[32]
1610	δNH_2	[53]
1612vs	$\nu_3(\delta NH)a_1+\nu_{15}(\delta NH)_{b2}$	[54]
1615	δNH_2	[46]
1615s	δNH	[55]
1617s	δNH_2	[32]
1628	δNH_2	[47]
3275	νNH_2	[32]
3380	$\nu_{as}NH_2$	[32]

3.4. FTIRRAS of gold in aqueous 0.1 M TU+0.5 M sulphuric acid

FTIRRAS spectra of gold in aqueous 0.1 M TU+0.5 M sulphuric acid were obtained taking $E_{ref} = 0.24$ V and collecting spectra by 0.05 V decreasing the potential stepwise from E_{ref} to −0.1 V and in reverse from −0.1 V to 1.5 V, using either p- or s-polarised light. It should be noted that 0.24 V is a potential slightly lower than

Table 2
Comparison of IR absorption bands (cm^{-1}) of solid sample of TU [53,56], copper–TU [33], silver–TU [57] and gold–TU (this paper) complex salts

TU	Ag(TU)	$Cu_2(TU)_5$	$Au(TU)_2$	$Cu_2(TU)_6$	$Cu_4(TU)_7$	Assignment
728s	718m	735	712m	700m	709m	νCS
1082m	1103s	1105	1105s	1075, 1104s	1052	νCN, ρNH_2
	1182w		1194m		1089m	
1410s	1389, 1424s	1448	1391, 1424s	1420s	1391, 1434s	ν(CN),νCS, ρNH_2
1472s	1481m		1478m	1524w	1467, 1495m	νCN
1615s	1603, 1634s	1612, 1698	1607, 1634s	1629s	1615, 1629s	δNH_2, δOH_2

$E_{rest} = 0.26$ V, the rest potential of gold in the working solution.

When E is decreased stepwise from E_{ref} to -0.1 V (Fig. 6), p-polarised light spectra exhibit only broad negative bands at 1200 and 1650 cm^{-1} related to bisulphate ion and water species. In contrast, at potentials positive to $E_{ref} = 0.24$ V, several features appear in the range 1300–1700 cm^{-1}, which start to be developed at approximately 0.35 V. The positive bands at 1405 and 1484 cm^{-1} coincide with those reported for TU at the copper | aqueous borax [27] and platinum | aqueous sulphuric acid [23] interface. The band at 1405 cm^{-1} has been assigned to symmetric N–C–N and C–S bond stretching, and NH_2 rocking modes in TU [23,32,34], while the band at 1487 cm^{-1} corresponds to the asymmetric C–N stretching and NH_2 bending modes of TU [23,32,34]. Thus, TU molecules are consumed and the product formed is responsible for the negative band at 1435 cm^{-1}. This frequency, however, can be assigned to active groups

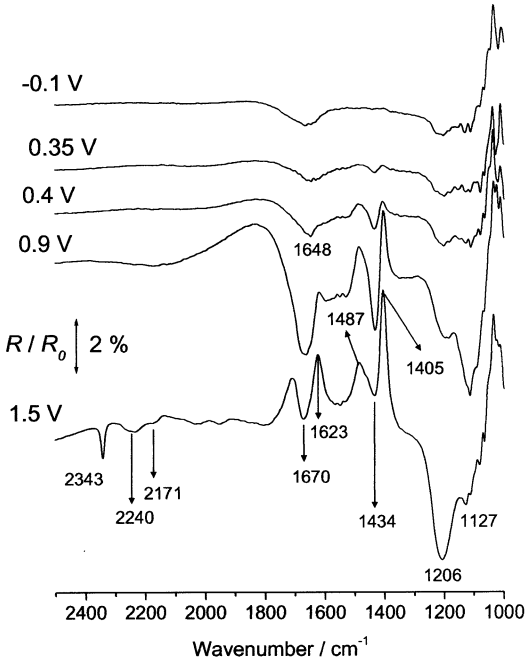

Fig. 6. p-Polarised light FTIRRAS spectra of gold in 0.1 M TU+0.5 M sulphuric acid at different potentials. $E_{ref} = 0.24$ V.

present in the TU molecule, and taking into account that at these potentials metal dissolution occurs [34], the product formed can be related to a gold–TU soluble complex according to

$$Au(s) + 2TU(aq) \rightarrow [Au(TU)_2]^+(aq) + e^- \quad (1)$$

As gold in TU-containing solutions undergoes chemical or electrochemical dissolution [7,24,35,36] forming $[Au(TU)_2]^+$ complex ions [10,11], it seems reasonable to assign the 1405/1434 cm^{-1} bipolar band to the appearance/disappearance of TU from the solution due to the formation of the gold complex. Accordingly, the band at 1434 cm^{-1} is due to the soluble gold complex in aqueous sulphuric acid. This conclusion is supported by the band at 1434 cm^{-1} in the spectrum of solid $[Au(TU)_2]_2SO_4$ (Fig. 5). The blue-shift of these bands as compared to those of TU indicates an increase in the C–N and C–S bond stretching vibration energy due to the greater double bond character of the C–N bond, and a decrease in the C–S bond order. This is consistent with the formation of a strongly polar sulphur–metal bond in the complex species. It should be noted that the blue-shift of the C–N and C–S bands of TU has also been observed in solid copper–TU complexes [33], as well as during copper dissolution in TU-containing aqueous borax, where copper–TU complex is formed [27]. The positive band at 1623 cm^{-1} corresponds to the bending scissoring of the NH_2 group of TU (Table 1).

The negative band at approximately 1648 cm^{-1} for $E = 0.4$ V (Fig. 6) correlates with the appearance of the positive bands at 1405 and 1484 cm^{-1}. The wide feature near 1648 cm^{-1} shifting to 1673 cm^{-1} as E is increased to 1.5 V can be assigned to the formation of FDS in solution (see Fig. 4b and Table 3). This band can be assigned to the bending of NH_2 in the molecule of FDS [23,32]. According to this assignment, soluble FDS would be formed for $E > 0.3$ V, i.e. during the development of peak Ia in the voltammogram (Fig. 1). However, water features can interfere in this frequency region, and therefore, for a definite identification of FDS absorption bands, FTIRRAS experiments performed in deuterium oxide solution are required, as described in Section 3.6.

The negative bands at 1127 and 1200 cm^{-1} (Fig. 6) are related to sulphate and bisulphate ion species [37],

Table 3
Principal infrared bands of FDS

Frequency/cm^{-1}	Assignment	References
1055	$\rho NH_2 + \nu_{as}CN_2$	[32]
1095	$\rho NH_2 + \nu_{s}CN_2$	[32]
1400	$\nu_{s}NCN + \rho NH_2 + \nu CS$	[32]
1585	$\delta NH_2 + \nu_{as}CN_2$	[32]
1630	$\delta NH_2 + \nu_{as}CN_2$	[32]
1654	δNH_2	[32]
1650	–	[23]

respectively. As E is changed from 0.4 to 0.9 V, the intensity of the band at 1127 cm^{-1} increases faster than that at 1200 cm^{-1}, although the latter suddenly increases for $E = 1.5$ V. The relative change in intensity of these bands can be caused by the formation of sulphate species from the complete electro-oxidation of TU at 1.5 V, and the simultaneous local acidification of the solution accompanying the formation of the oxygen-containing layer on gold from water electro-oxidation. Although hydrogen ions from the anodisation process in part migrate outwards, another part is neutralised by sulphate ion migration inwards. The enrichment of anions at the interface is reflected in the increase in the sulphate band intensity [38]. To discriminate between bands coming from the TU electro-oxidation process and those associated with solution components, runs in aqueous perchloric acid were made (next section).

Finally, the spectrum recorded for $E = 1.5$ V (Fig. 6) shows other negative bands at 2343, 2171 and 2240 cm^{-1}. The band at 2343 cm^{-1} corresponds to the O–C–O asymmetric stretching [39] and reveals the formation of carbon dioxide from late TU electro-oxidation. The bands at 2171 and 2240 cm^{-1} would indicate the formation of CN-compounds since the C≡N stretching band for pure cyanamide is located at 2280 cm^{-1} [40] and for benzonitrile at 2235 cm^{-1} [41]. Cyanamide has been found as a product of TU electro-oxidation on platinum [22,23]. It should be noted, however, that the hydrolysis of nitriles in acid would yield the corresponding amide. The latter should exhibit a band at approximately 1660 cm^{-1} due to the C=O stretching [41] that, in our case, would probably be obscured by the bands corresponding to water and FDS in this range of spectra.

Spectra run with s-polarised light, and a high angle of incidence, which provides only information on species in solution, are much less sensitive than spectra obtained with p-polarised light [38]. In our case, spectra obtained with s-polarised light show the same bands already observed with p-polarised light, although with a poorer definition.

3.5. FTIRRAS of gold in 0.1 M aqueous TU+perchloric acid

To study the electrosorption and electro-oxidation of TU in the potential range of FDS formation and incipient gold electrodissolution, FTIRRAS spectra in perchloric acid solutions were run immersing the electrode either at $E_i = E_{ref} = -0.1$ V and increasing E stepwise from -0.1 up to 0.3 V, or at $E_i = E_{ref} = 0.3$ V and decreasing E stepwise down to -0.1 V.

For $E_{ref} = -0.1$ V, i.e. at a potential below that corresponding to the electro-oxidation of TU to FDS, the stepwise increase in E from -0.1 to 0.1 V produces no significant change in the spectra over the region 1000–1600 cm^{-1}. However, for E above 0.15 V, positive bands at 1405 and 1487 cm^{-1}, and negative bands at 1430, 1528 and 1642 cm^{-1} begin to be observed (Fig. 7). The intensity of these bands increases as E is shifted positively.

On the other hand, starting from $E = 0.3$ V and decreasing E stepwise to -0.1 V, the spectra show negative bands at 1405 and 1487 cm^{-1}, and positive bands at 1430, 1528 and 1642 cm^{-1}, the intensity of all these bands increasing as E is decreased (Fig. 8). The s-polarised light spectra (not shown) exhibited the same

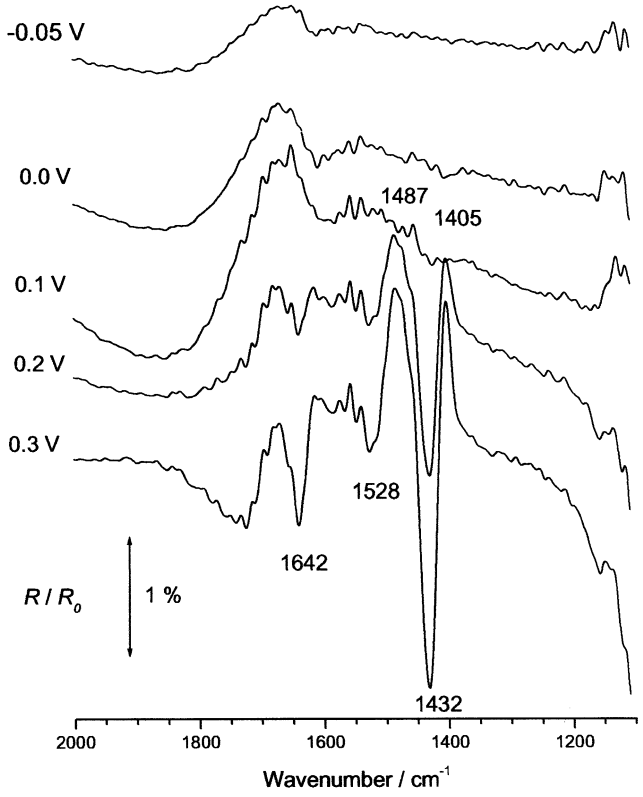

Fig. 7. p-Polarised light FTIRRAS spectra of gold in aqueous 0.1 M TU+0.5 M perchloric acid at different sampling potentials. The electrode was immersed at $E_i = -0.1$ V (E_{ref}) and the potential increased stepwise.

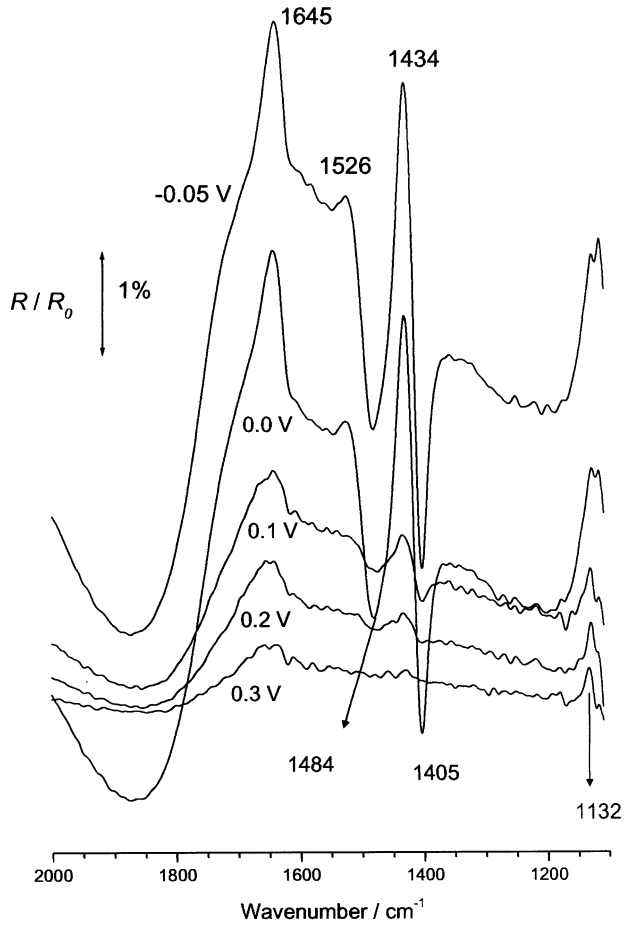

Fig. 8. p-Polarised light FTIRRAS spectra of gold in aqueous 0.1 M TU+0.5 M perchloric acid at different sampling potentials. The electrode was immersed at $E_i = 0.3$ V (E_{ref}) and the potential decreased stepwise.

bands confirming that all of them are related to species in solution.

The behaviour of the spectra when the electrode potential is either increased or decreased in the range −0.1–0.3 V indicates that the same reactions proceeds when the potential direction is reversed.

The bands at 1480 and 1528 cm^{-1} show the formation of TU (1480 cm^{-1}), and the disappearance of the soluble gold complex (1528 cm^{-1}) (Fig. 8). This band shift agrees with data reported for copper–TU complexes [27,33]. The blue-shift of the band at 1480 cm^{-1} is accompanied by a decrease in intensity and the appearance of weaker bands at 1524–1514 cm^{-1} [27,33].

Finally, the negative band at approximately 1642 cm^{-1} (Fig. 8) appears for $E > 0.15$ V, its intensity increasing as E is changed from 0.3 to −0.1 V and vice versa. Accordingly, this band should be related to soluble species that are produced at potentials more positive than 0.15 V, in agreement with voltammetric results (Fig. 1). The band at 1642 cm^{-1} should be related to the bending of the NH_2 group of FDS [23,32], the first electro-oxidation product of TU on platinum [19,30], copper [20], gold [16,36] and silver [28] electrodes. The presence of FDS bands was confirmed by running spectra in deuterium oxide as shown further on.

This set of experiments allowed us to conclude that for E increasing from −0.1 to 0.3 V, both the soluble gold complex and FDS species are formed. These products can be electroreduced to TU by decreasing E backwards to −0.1 V. This behaviour agrees with the presence of the conjugated peaks Ia/Ic in the voltammograms within the same potential range (Fig. 1).

As E is increased from 0.3 to 0.9 V (Fig. 9), the intensity of the negative bands at 1120 cm^{-1} due to perchlorate ions increases because of the local accumulation of these ions at the positively charged gold surface. Simultaneously, the intensity of both the positive bands at 1405 and 1483 cm^{-1} related to the depletion of TU, and the negative bands at 1434 and 1530 cm^{-1}, related to soluble gold complex increases as E is shifted positively, can be observed.

On the other hand, the complex band in the region 1600–1700 cm^{-1} consists of two negative bands centred at 1640 and 1690 cm^{-1} and a minimum at 1660 cm^{-1}, probably associated with a positive band. The intensity of these negative bands also increases with E, in contrast to the intensity of the minimum at 1660 cm^{-1} that tends to disappear (Fig. 9).

For $E > 1.2$ V, i.e., at potentials related to the formation of the oxygen-containing layer on gold, the spectra in the 1000–2500 cm^{-1} region (Fig. 9) exhibit negative bands at 1120 and 1200 cm^{-1} corresponding to sulphate and bisulphate, their intensity increasing as E is shifted positively. For $E = 1.5$ V the band at 1200 cm^{-1} increases at the expense of the band at 1120 cm^{-1}. These results indicate that the formation of sulphate ions from TU electro-oxidation occurs in the potential range where the formation of the oxygen-containing layer on gold takes place. Presumably, the local acidification caused by the anodisation modifies the sulphate/bisulphate concentration ratio at the thin layer of solution. This would explain the evolution of spectra with E at such potentials.

It should be noted that the negative band at 1127 cm^{-1}, exhibiting something like a hump at 1100 cm^{-1}, is actually a complex band involving the absorption of both sulphate and perchlorate ions. The major contribution to this complex band comes from perchlorate ions that migrate from the bulk to the thin layer of solution in contact with the electrode, increasing the local concentration of these ions progressively with E. The increasing migration of perchlorate ions from the bulk towards the electrode surface is required to balance the positive charge flow due to the formation of positive ions such as the gold–TU complex and protons, the latter being produced during the formation of the oxygen-containing layer on gold. Besides, the step

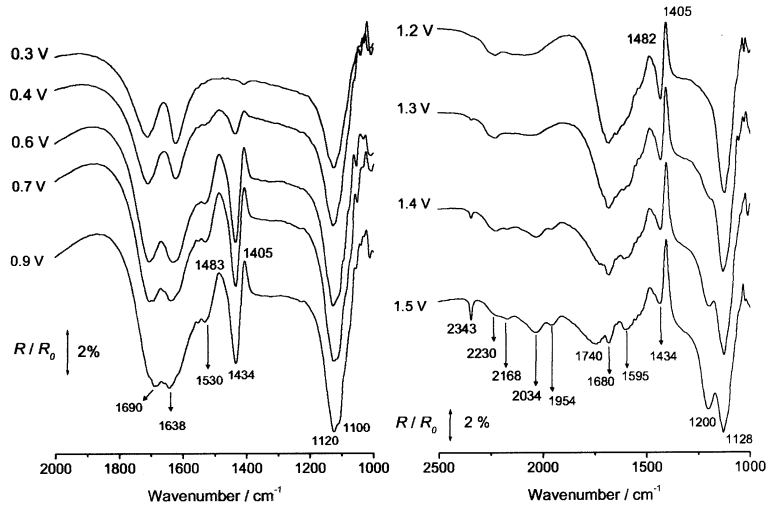

Fig. 9. p-Polarised light FTIRRAS spectra of gold in aqueous 0.1 M TU+0.1 M perchloric acid at different sampling potentials. $E_{ref} = 0.24$ V.

between sampling potentials also causes a charge to pass from the working to the auxiliary electrode, which is transported by ions migrating between the thin layer cavity and the bulk of the electrolyte [41,42]. On the other hand, the depletion of TU can be followed through the potential-dependent intensity of the positive bands at 1405 and 1485 cm^{-1}, although this is not feasible with the negative band at 1435 cm^{-1} that is rather insensitive to changes in E. The different E dependences of these bands suggests that the electro-dissolution of gold as a complex species is dumped by an increasing passivation of the gold surface. Passivation occurs at potentials where sulphate, carbon dioxide and CN-containing species are formed.

As E is increased to 1.5 V, a broad asymmetric feature is observed in the region 1500 and 1800 cm^{-1}, which develops into two bands centred at 1680 cm^{-1}. Also the development of a new band at 1740 cm^{-1} can be observed (Fig. 9b).

For $E \geqslant 1.3$ V, the band at 2343 cm^{-1} confirms the formation of carbon dioxide and the small negative bands observed in the range 1800–2500 cm^{-1} can be assigned to the formation of C≡N-containing species, probably cyanamide [23].

When E exceeds the threshold potential for water electro-oxidation on gold an oxygen-containing layer according to

$$Au + H_2O \rightarrow Au(OH)_{ad} + H^+ + e^- \quad (2)$$

$$Au(OH)_{ad} \rightarrow Au(O)_{ad} + H^+ + e^- \quad (3)$$

is formed first, followed by gold oxide formation when $E > 1.2$ V [43–45].

Then, OH/O species contribute to the formation of both carbon dioxide and sulphate/bisulphate species from TU and TU byproducts. Adsorbed TU byproducts such as FDS and S have been observed by STM imaging on Au (1 1 1) [25] at potentials above 0.3 V, and detected by XPS and FTIRRAS for Ag (1 1 1) [28].

Thus, the results obtained either in sulphuric or perchloric acid solutions indicate that TU electro-oxidation at potentials up to 1.5 V results in the formation of both O- and CN-containing products.

Spectra recorded with s-polarised light exhibit the same bands observed with p-polarised light spectra, indicating that all the observed bands are related to the formation or depletion of species in solution.

3.6. FTIRRAS spectra of gold in 0.1 M TU+0.1 M sulphuric acid in D_2O

To diminish the interference of water and to avoid as much as possible that from the acid, p and s spectra using 0.1 M TU+0.1 M sulphuric acid in deuterium oxide, in the range 0.3–1.5 V and $E_{ref} = 0.2$ V were obtained. In deuterated acid solutions both TU and FDS amine hydrogens are readily exchanged with deuterium from the solvent [46]. As a result, absorption bands for deuterated TU appear at 1388 and 1519 cm^{-1} [23,47], and for deuterated FDS at 1399 and 1631 cm^{-1} [23] (Table 4).

The p-polarised light spectra run from 0.3 to 0.9 V (Fig. 10) show positive bands at 1343, 1382 and 1516 cm^{-1}, and negative bands at 1236, 1395, 1560 and 1632 cm^{-1}. Bipolar bands are defined by the pair of peaks at 1382/1395 cm^{-1} and 1516/1560 cm^{-1}. The positive bands at 1382 and 1516 cm^{-1} are assigned to the depletion of deuterated TU, and the band at 1395 cm^{-1} to the appearance of deuterated FDS [23] that can already be seen for $E = 0.4$ V. The negative band at 1632 cm^{-1}, which has also been assigned to deuterated FDS [23], appears for $E \geqslant 0.6$ V. Moreover, for $E = 1.5$ V, the intensity of the band at 1398 cm^{-1} tends to decrease, while that of the band at 1632 cm^{-1} increases con-

Table 4
Principal infrared bands of deuterated TU and FDS

Frequency/cm^{-1}	Assignment	References
1390 (TU)	$\nu_s CN_2$	[29]
1474 (TU)	$\nu_{as} CN_2$	[29]
1190 (TU)	δND_2	[29]
1140 (TU)	δND_2	[29]
1131 (TU)	δND_2	[58]
1284 (TU)	δND_2	[58]
1355 (TU)	$\nu_s C-N$	[58]
1449 (TU)	$\nu_{as} C-N$	[58]
1388 (TU)	δND_2	[47]
1507 (TU)	δND_2	[47]
1399 (FDS)		[23]
1631 (FDS)		[23]

tinuously (Fig. 10). The apparent lower intensity of the positive band at 1398 cm^{-1} is probably due to the enhancement of the TU band at 1382 cm^{-1} that shifts the FDS band upwards.

The new negative band at 1560 cm^{-1} and the positive band at 1516 cm^{-1} constitute a bipolar band presumably associated with the appearance of the gold complex and the disappearance of TU. Therefore, there is a red shift of the bands related to the bending of the NH_2 groups caused by deuteration. As E is increased beyond 1.2 V, the negative band at 1562 cm^{-1} disappears and a new small negative band at 1587 cm^{-1} can be seen.

On the other hand, the negative band at 1236 cm^{-1} is the only potential-dependent band, as it shifts from approximately 1236 to 1252 cm^{-1} when E increases from 0.8 to 1.5 V. Bisulphate ions formed in solution are responsible for the high intensity of this band. However, overlapping with a surface feature causes the band centre to shift with E. The latter is likely to be associated with an adsorbed species with a shift of 27 cm^{-1} V^{-1}. This shift is comparable to that observed for sulphate on polycrystalline platinum (20–30 cm^{-1} V^{-1}) [37] and lower than the 85 cm^{-1} V^{-1} observed for gold (1 1 1) [48] or the 40–58 cm^{-1} V^{-1} for platinum (1 0 0) [49]. For gold (1 1 1), FTIRRAS spectra of adsorbed sulphate exhibit a prominent SO stretching band between 1155 and 1220 cm^{-1}, depending on the applied potential [48]. The frequency shift of adsorbed sulphate from that corresponding to the solution phase species is a feature usually expected from the change of symmetry produced upon adsorption [50].

The major adsorption of bisulphate ions on gold can be discarded because at high positive potentials, the bisulphate ion is polarised concentrating the electron density towards the electrode surface. Then, the oxygen atoms that are away from the electrode surface become less negatively charged increasing the acid character of bisulphate. Consequently, any adsorbed bisulphate ion tends to dissociate on the surface into adsorbed sulphate and hydrogen ions that migrate outwards [49]. This is consistent with previous FTIR data for gold (1 1 1) in sulphate/bisulphate solutions that showed the absence of bisulphate species on the metal surface [48].

It should be noted that the appearance of adsorbed sulphate is observed in the potential range related to the electro-oxidation of TU to sulphate assisted by the initial stage of water discharge on gold yielding OH and O adsorbed species (Eq. (2)). Sulphate adsorption on gold produces ordered structures [48,51] and brings about changes in surface relaxation and surface stress of the gold surface [52].

s-Polarised light spectra exhibit all but the negative band at 1236 cm^{-1} observed for p-polarised light

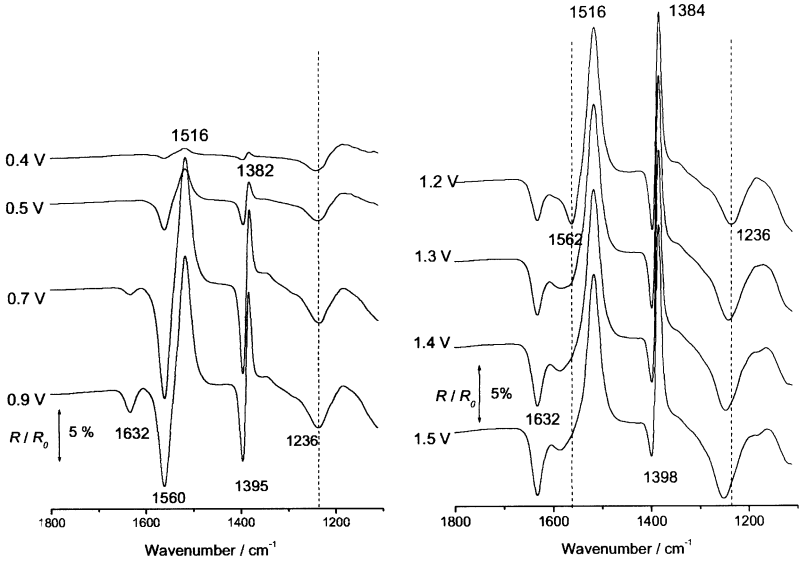

Fig. 10. p-Polarised light FTIRRAS spectra of gold in deuterium oxide 0.1 M TU + 0.1 M sulphuric acid at different sampling potentials. $E_{ref} = 0.2$ V.

spectra. This indicates that, except the adsorbed sulphate, all the rest of the species detected are in solution.

4. Conclusions

(1) The voltammetric electro-oxidation of TU on gold for $c_{TU} = 0.1$ M involves two main consecutive stages characterised by anodic peaks at approximately 0.5 and 1.0 V, related to the formation of FDS and the electrodissolution of gold as gold–TU complex ions.

(2) FTIRRAS spectra allow monitoring the electro-oxidation reaction of both gold and TU through the appearance of loss and gain bands related to the gold complex and TU byproduct species.

(3) According to FTIRRAS spectra, gold electrodissolution starts at approximately $E = 0.15$ V and increases as E is increased. The soluble gold–TU complex is electroreduced when E is decreased from 0.15 V.

(4) The electro-oxidation of TU and the electrodissolution of gold are concomitant processes that at potentials below 0.9 V produce FDS and $[Au(TU)_2]^+$ soluble species. The formation and electroreduction of these species are complementary processes.

(5) In the potential range related to the first water discharge step on gold, the main electro-oxidation products are carbon dioxide, sulphate and CN-containing species. The formation of O-containing products from TU and TU byproducts is assisted by OH and O adsorbates on the gold surface and gold oxide produced from water discharge.

(6) For $E > 1.2$ V, both adsorbed and soluble sulphate species are formed. Adsorbed sulphate exhibits a band shift of 27 $cm^{-1}\,V^{-1}$. Local acidification at the anodic interface presumably modifies the sulphate/bisulphate concentration ratio.

Acknowledgements

This work was supported financially by the Consejo Nacional de Investigaciones Científicas y Técnicas (CONICET), Agencia Nacional de Promoción Científica y Tecnológica (PICT 98 06-03251) of Argentina and the Comisión de Investigaciones Científicas de la Provincia de Buenos Aires (CIC).

References

[1] K.C. Pillai, R. Narayan, J. Electrochem. Soc. 125 (1978) 1393.
[2] A.S.M.A. Haseeb, P.L. Schilardi, R.C.V. Piatti, A.E. Bolzán, R.C. Salvarezza, A.J. Arvia, J. Electroanal. Chem. 500 (2001) 543.
[3] L.M. Gassa, J. Lambi, A.E. Bolzán, A.J. Arvia, J. Electroanal. Chem. 32 (2002) 71.
[4] K. Sykut, J. Saba, B. Marczewska, G. Daimata, J. Electroanal. Chem. 178 (1984) 295.
[5] R.M. Souto, S. Gonzáles, A. Arévalo, J. Electroanal. Chem. 216 (1987) 273.
[6] A. Szymaszek, J. Biernat, L. Pajdowski, Electrochim. Acta 22 (1977) 359.
[7] I.N. Plaksin, M.A. Kozhukhova, C.R. Acad. Sci. USSR 31 (1941) 671.
[8] T. Groenewald, Hydrometallurgy 1 (1976) 277.
[9] G. Deschènes, E. Ghali, Hydrometallurgy 20 (1988) 179.
[10] L.C. Porter, J.P. Fackler, J. Costamagna, R. Schmidt, Acta Cryst. C48 (1992) 1751.
[11] O.E. Piro, E.E. Castellano, R.C.V. Piatti, A.E. Bolzán, A.J. Arvia, Acta Cryst. C58 (2002) 252.
[12] B.H. Loo, Phys. Lett. 89 (1982) 346.
[13] M. Fleischmann, I.R. Hill, G. Sundholm, J. Electroanal. Chem. 157 (1983) 359.
[14] R. Holze, S. Shomaker, Electrochim. Acta 35 (1990) 613.
[15] A.E. Bolzán, R.C.V. Piatti, R.C. Salvarezza, A.J. Arvia, J. Appl. Electrochem. 32 (2002) 611.
[16] A.E. Bolzán, R.C.V. Piatti, A.J. Arvia, J. Electroanal. Chem., in press.
[17] P. Gao, M.L. Patterson, M.A. Tadayyoni, M.J. Weaver, Langmuir 1 (1985) 173.
[18] H. Wroblowa, M. Green, Electrochim. Acta 8 (1963) 679.
[19] A.E. Bolzán, I.B. Wakenge, R.C. Salvarezza, A.J. Arvia, J. Electroanal. Chem. 475 (1999) 181.
[20] A.E. Bolzán, I.B. Wakenge, R.C.V. Piatti, R.C. Salvarezza, A.J. Arvia, J. Electroanal. Chem. 501 (2001) 241.
[21] P.W. Preisler, L. Berger, J. Am. Chem. Soc. 69 (1947) 322.
[22] P.C. Gupta, Z. Anal. Chem. 196 (1963) 412.
[23] M. Yan, K. Liu, Z. Jiang, J. Electroanal. Chem. 408 (1996) 225.
[24] T. Groenewald, J. Appl. Electrochem. 5 (1975) 71.
[25] O. Azzaroni, B. Blum, R.C. Salvarezza, A.J. Arvia, J. Phys. Chem. B 104 (2000) 1395.
[26] J.O.M. Bockris, M.A. Habib, J.L. Carbajal, J. Electrochem. Soc. 131 (1984) 3032.
[27] S.N. Port, S. Ceré, D.J. Schiffrin, J. Electroanal. Chem. 432 (1997) 215.
[28] V. Brunetti, B. Blum, R.C. Salvarezza, A.J. Arvia, P.L. Schilardi, A. Cuesta, J. Gayone, G. Zampieri, J. Phys. Chem. B 106 (2002) 9831.
[29] D. Papapanayiotou, R.N. Nuzzo, R.C. Alkire, J. Electrochem. Soc. 145 (1998) 3366.
[30] S.J.J. Reddy, V.N. Krishnan, J. Electroanal. Chem. 27 (1970) 473.
[31] V. Gaspar, A.S. Mejerovich, M.A. Meretukov, J. Schmiedl, Hydrometallurgy 34 (1994) 369.
[32] G. Peyronel, W. Malavasi, A. Pignedoli, Spectrochim. Acta 39A (1983) 617.
[33] R.C. Bott, G.A. Bowmaker, C.A. Davis, G.A. Hope, B.E. Jones, Inorg. Chem. 37 (1998) 651.
[34] S.N. Port, S.L. Horswell, R. Raval, D.J. Schiffrin, Langmuir 12 (1996) 5934.
[35] R.G. Schulze, J. Metals (1984) 62.
[36] H. Zhang, I.M. Ritchie, S.R.L. Brooy, J. Electrochem. Soc. 148 (2001) D146.
[37] K. Kunimatsu, M. Samant, H. Seki, M.R. Philpott, J. Electroanal. Chem. 243 (1988) 203.
[38] T. Iwasita, F. Nart, in: H. Gerischer, C.W. Tobias (Eds.), Advances in Electrochemical Science and Engineering, vol. 4, VCH, Weinheim, 1995, p. 123.
[39] G. Herzberg, Molecular Spectra and Molecular Structure II: Infrared and Raman Spectra of Polyatomic Molecules, Van Nostrand Reinhold, New York, 1945.
[40] C.J. Pouchert, The Aldrich Library of Infared Spectra, third ed., Aldrich Chemical Co, Milwakee, 1981.
[41] A. Chen, J. Richer, S.G. Roscoe, J. Lipkowski, Langmuir 13 (1997) 4737.

[42] N.S. Marinkovič, J.J. Calvente, Z. Kovčov, W.R. Fawcett, J. Electrochem. Soc. 143 (1996) L171.
[43] H. Angerstein-Kozlowska, B.E. Conway, B. Barnett, J. Mozota, J. Electroanal. Chem. 100 (1979) 417.
[44] H. Angerstein-Kozlowska, B.E. Conway, A. Hamelin, L. Stoicoviciu, Electrochim. Acta 31 (1986) 1051.
[45] C.M. Ferro, A.J. Calandra, A.J. Arvia, J. Electroanal. Chem. 65 (1975) 963.
[46] D. Hadžic, J. Kidrič, Z.K. Kneževic, B. Barlič, Spectrochim. Acta A 32 (1976) 693.
[47] G.B. Aitken, J.L. Duncan, G.P. McQuillan, J. Chem. Soc. A (1971) 2695.
[48] G.J. Edens, X.P. Gao, M. Weaver, J. Electroanal. Chem. 375 (1994) 357.
[49] F.C. Nart, T. Iwasita, M. Weber, Electrochim. Acta 39 (1994) 2093.
[50] F.C. Nart, T. Iwasita, J. Electroanal. Chem. 322 (1992) 289.
[51] O.M. Magnussen, J. Hegebock, J. Hotlos, R.J. Behm, Faraday Discuss. (1992) 329.
[52] R.J. Nichols, T. Nouar, C.A. Lucas, W. Haiss, W.A. Hofer, Surf. Sci. 513 (2002) 263.
[53] A. Yamaguchi, P.B. Penland, S. Mizushima, T.J. Lane, C. Curran, J.V. Qualgiano, J. Am. Chem. Soc. 80 (1958) 527.
[54] J. Stewart, J. Chem. Phys. 26 (1957) 248.
[55] R. Rivest, Can. J. Chem. 40 (1962) 2234.
[56] M.M. El-Etri, W.M. Scovell, Inorg. Chem. 29 (1990) 480.
[57] S.N. Cesaro, Vibrational Spectroscopy 16 (1998) 55.
[58] L. Bencivenni, S.N. Cesaro, A. Pieretti, Vibrational Spectroscopy 18 (1998) 91.